Molecular Biology, Vol. 36, No. 3, 2002, pp. 400–411. Translated from Molekulyarnaya Biologiya, Vol. 36, No. 3, 2002, pp. 511–524.

STRUCTURAL–FUNCTIONAL ANALYSIS OF POLYMERS AND THEIR COMPLEXES

UDC 577.323

Interaction of Topotecan, DNA Topoisomerase I Inhibitor, with Double-stranded Polydeoxyribonucleotides. 3. Binding at the Minor Groove

S. A. Strel'tsov[1], A. L. Mikheikin[1], S. L. Grokhovsky[1, 2], V. A. Oleinikov[3], and A. L. Zhuze[1]

[1] *Engelhardt Institute of Molecular Biology, Russian Academy of Sciences, Moscow, 119991 Russia; E-mail: strelcov@imb.ac.ru*

[2] *University of Oslo Medical Research Center, Moscow, 117334 Russia*

[3] *Shemyakin–Ovchinnikov Institute of Bioorganic Chemistry, Russian Academy of Sciences, Moscow, 117871 Russia*

Received May 21, 2001

Abstract—Interaction of topotecan (TPT) with calf thymus DNA, coliphage T4 DNA, and poly(dGdC)·poly(dG-dC) was studied by optical (linear flow dichroism, UV-vis spectroscopy) and quantum chemical methods. The linear dichroism signal of TPT bound to DNA was shown to have positive sign in the range 260–295 nm. This means that the plane of quinoline fragment (rings A and B) of TPT forms an angle less than 54° with the long axis of DNA, and hence the TPT molecule cannot intercalate between DNA base pairs. TPT was established to bind to calf thymus DNA as readily as to coliphage T4 DNA whose cytosines in the major groove were all glycosylated at the 5th position. Consequently, the DNA major groove does not participate in TPT binding. TPT molecule was shown to compete with distamycin for binding sites in the minor groove of DNA and poly(dG-dC)·poly(dG-dC). Thus, it was demonstrated for the first time that TPT binds to DNA at its minor groove.

Key words: DNA topoisomerase I, camptothecin, topotecan, DNA minor groove, linear flow dichroism, quantum chemical calculation

INTRODUCTION

This study is a continuation of a series of papers dealing with the interaction of topotecan (water-soluble camptothecin derivative), human DNA topoisomerase I inhibitor, with double-helical polydeoxyribonucleotides (previous communication see [1]). Alkaloid camptothecin (CPT) from *Camptotheca acuminata* was isolated in 1966 [2]. CPT was found to inhibit rapidly and efficiently the synthesis of nucleic acids in eukaryotic cells, although it did not interact directly with enzymes participating in DNA or RNA biosynthesis [3]. Subsequent studies have established that CPT binds to DNA–DNA topoisomerase I (topo I) covalent complex, weakly adsorbs on linear DNA [4–6], and does not interact with isolated topo I [7]. Although the interaction of CPT and its analogs with DNA is studying longer than twenty five years, their localization on DNA is still unknown. A number of authors supposes CPT and its derivatives to be intercalated between DNA base pairs [4, 6, 8, 9]. These authors argue that the interaction of molecules of this family with DNA results in induced CD of negative sign and hypochromism of the long-wavelength, not overlapping with DNA, absorption band of the ligand [4, 6]. One of the models of DNA/topo I/CPT triple complex suggests that CPT molecules intercalate between DNA base pairs [10]. An angle between the long-wavelength electron transition dipole moments (ETDM) of bound CPT molecule and the long axis of DNA was determined by electrical linear dichroism to reveal the orientation of CPT molecule with respect to DNA base pairs. It proved to be 57°–59° [11]. This angle value is intermediate between the angles for known intercalators, 62°–76° [12], and angles <55° characteristic of molecules localized in the DNA minor groove [13]. Therefore the authors of work [11] are disposed to think that CPT binds to DNA in the major groove because CPT binding to DNA causes induced CD of negative sign in CPT absorption band, whereas it is known that molecules bound at the minor groove as a rule have positive sign of induced CD [14]. The authors of [6, 15] also suppose CPT family molecules to be localized in the DNA major groove.

0026-8933/02/3603-0400$27.00

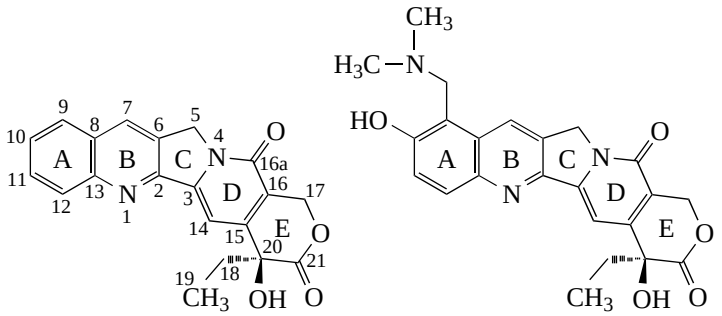

Fig. 1. Chemical structure of camptothecin and topotecan.

Topotecan (TPT, NSC609699) is a CPT analog (see Fig. 1) used in clinic under the name of hycamtin in the treatment for a number of oncological diseases [10]. It is readily soluble in water, which facilitates its physicochemical studies. We have shown recently that, on the one hand, TPT molecules (see Fig. 1) form dimers in solution [16], and on the other hand, DNA molecules acquire ability to interact with each other when combine with TPT [1]. The aim of this work is to determine the localization of TPT on DNA. We used linear flow dichroism (LD). This method detects only TPT molecules bound to DNA, which is very important for such weakly interacting with DNA ligands as CPT and its analogs. On the other hand, this method enables one to determine the orientation of the quinoline chromophore plane (rings A-B) of TPT molecule with respect to the long axis of DNA, i.e., to the plane of its base pairs.

We showed recently, that TPT formed several types of complexes with DNA in solutions of low ionic strength [1]. It should be noted that similar conclusion about CPT molecules was made even in paper [4], but it was based upon the curvature of adsorption isotherm. According to [17, 18], such interpretation would be unambiguous only if CPT molecule occupies one base pair on DNA, but this was not shown in these works.

We have established that TPT is localized in the DNA minor groove upon binding. This result pertains only to TPT–DNA complex that has negative LD_{390}.

EXPERIMENTAL

Materials. Topotecan from SmithKline Beecham was kindly provided by Professor I.R. Nabiev, it was purified and analyzed for homogeneity as described in [16]. Sodium cacodylate, calf thymus DNA, and coliphage T4 DNA were from Sigma. Distamycin A (Dst) from Serva was used without additional purification. The concentration of initial Dst solution was $1.08 \cdot 10^{-4}$ M. It was dissolved in a 1:1 (vol.) methanol–dimethylsulfoxide mixture. We used poly(dG-dC)·poly(dG-dC) from P.-L. Biochemicals. Both DNAs and poly(dG-dC)·poly(dG-dC) were dissolved in 1 mM sodium cacodylate buffer, pH 6.8, followed by dialysis at 4° against the same buffer with its triple replacement. The duration of dialysis stage was at least 12 h, the ratio of DNA/buffer solution volumes in the dialysis was 1:15. The concentrations of calf thymus DNA, poly(dG-dC)·poly(dG-dC), coliphage T4 DNA, and Dst were determined spectrophotometrically using molar extinction coefficients: ε_{260} = 6600, ε_{253} = 8400, ε_{260} = 6800, ε_{303} = 34000 M^{-1} cm^{-1}, respectively [19–21]. The concentrations of DNAs and poly(dG-dC)·poly(dG-dC) are given in moles (bp) per liter.

The complexes of TPT with DNAs and poly(dG-dC)·poly(dG-dC) were prepared from concentrated solutions of polydeoxyribonucleotides ($\approx 1 \cdot 10^{-3}$ M) and a concentrated TPT solution ($1.8 \cdot 10^{-4}$ M). Optical measurements were performed in three days after complex preparation except for specially noted cases due to the low rate of DNA–TPT complex formation [1].

Spectral measurements. Absorption spectra were measured on a Cary 118 spectrophotometer. CD spectra were obtained on a Roussel–Jouan Jobin-Yvon Mark III dichrograph. LD spectra were recorded with the use of specially designed add-on unit to this dichrograph [22].

LD_λ is the difference in the absorption of light polarized parallel and perpendicular to the flow and is determined by the formula which is a function of three independent variables (α, S, A_λ) [23]:

$$LD_\lambda = (A_\parallel - A_\perp)_\lambda = 3/2(3\cos^2\alpha - 1)SA_\lambda, \qquad (1)$$

where $A_\parallel$, $A_\perp$, and A are the absorptions of light polarized parallel and perpendicular to the flow and of nonpolarized light, respectively, at wavelength λ; S is the factor of orientation ability of macromolecule in a flow, which depends on its length, rigidity, solvent vis-

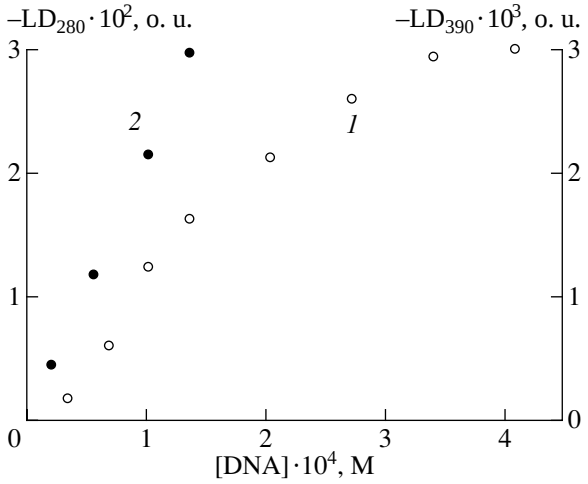

Fig. 2. Concentration dependence of LD of free DNA measured at 280 nm and of LD of TPT–DNA complex measured at 390 nm. TPT concentration is $1.05 \cdot 10^{-5}$ M. Curve *1*, TPT–DNA complex (right axis); curve *2*, free DNA (left axis). 1mM cacodylate buffer, pH 6.8. Average flow rate gradient is ~700 s^{-1}, optical path length of cuvette is 0.1 cm.

cosity, etc.; α is the angle between ETDM corresponding to light absorption at wavelength λ and flow direction. At flow rate gradients used (<700 s^{-1}), LD is observed only for sufficiently long double-stranded polynucleotides in a free state or as complexes with low-molecular ligands.

Below we will often use reduced LD (LD_r):

$$(LD_r)_\lambda = ((A_\parallel - A_\perp)_\lambda)/A_\lambda = 3/2(3\cos^2\alpha - 1)S. \quad (2)$$

Quantum chemical calculation of quinoline and lactone fragments of topotecan molecule. TPT molecule consists of two weakly bound with each other chromophore systems [24]. Therefore we used quinoline and lactone fragments of TPT molecule for quantum chemical calculations. The quinoline fragment consisted of rings A and B and contained methyl substituents at 2 and 6 positions, i.e., at the junction of ring B to ring C. The lactone fragment consisted of rings D and E and contained methyl substituents at 3 and 4 positions, i.e., at the junction of ring D to ring C. All quantum chemical calculations were performed using INDO/S method in vacuum [25].

RESULTS AND DISCUSSION

Does TPT intercalate between DNA base pairs? To answer this question, it is necessary to determine the angle between the plane of quinoline chromophore of TPT molecule and the long axis of DNA. For this purpose, preliminary we obtained a curve of TPT binding to DNA. Portions of concentrated DNA solution were added to $1.05 \cdot 10^{-5}$ M TPT solution, and LD was measured at 390 nm (in the long-wavelength absorption band of TPT) in the absence of overlapping with DNA absorption band. The dependence obtained is shown in Fig. 2, curve *1*. The fact of appearance of LD in the TPT absorption band (outside DNA absorption band) indicates TPT binding to DNA. The dependence obtained is an S-shaped curve and reaches saturation at DNA concentration about $3.5 \cdot 10^{-4}$ M, i.e., all TPT molecules prove to be bound to the polymer at this DNA concentration. For comparison, curve *2* in Fig. 2 shows concentration dependence of LD of free DNA measured at 280 nm. The latter dependence is linear. Thus, the S-shaped binding curve (Fig. 2, curve *1*) reflects just TPT binding to DNA. We analyzed this shape of curve for TPT binding to DNA in our previous paper [1].

LD and light absorption (A) spectra of TPT–DNA complex in the long-wavelength absorption band of TPT were measured at DNA concentration $3.5 \cdot 10^{-4}$ M and TPT concentration $1.05 \cdot 10^{-5}$ M. Then, LD_r spectrum was obtained with the use of formula (2). It has been shown above that all TPT is bound to DNA under these conditions (see Fig. 2, curve *1*). This condition is substantial because by definition $LD_r = LD/A$, where LD and A must refer only to bound ligand. LD value always refers to bound ligand. As a rule, both free and bound ligand make contribution to the absorption. Generally speaking, it is difficult to separate these contributions. Therefore LD_r was determined under conditions when all TPT was bound to DNA. Figure 3a shows absorption spectrum of bound TPT at concentration of $1.05 \cdot 10^{-5}$ M, Fig. 3b shows LD spectrum of TPT at the same concentration, and Fig. 3c shows LD_r spectrum of TPT. It should be noted that LD spectrum in this wavelength region has negative sign. According to formula (1), negative sign of LD indicates that corresponding ETDMs of bound TPT molecule form angle with the long DNA axis larger than 54°. We measured light absorption and LD at 280 nm of free DNA at several concentrations to determine the strict value of this angle. Then its LD_r was found using formula (2) to be 0.226 ± 0.007. DNA bases are known to form the angle of 70° with the long axis of DNA [12]. Therefore the value of S for free DNA may be calculated with the aid of formula (2). It proved to be 0.233 ± 0.007 under our experimental conditions. After that, assuming parameter S to be constant upon TPT–DNA complex formation, we calculated the angles between the long axis of DNA and long-wavelength ETDM in TPT molecule bound to DNA. They proved to be in the region of 62°–64°. It is interesting to note that virtually the same values of angle (57°–59°) between the long-wavelength ETDM in CPT molecule bound to DNA and the long axis of DNA were obtained in work [11].

It was shown earlier that association of several DNA molecules with each other took place upon inter-

action of TPT with DNA [1]. In this case, it is reasonable to suppose that the orientation ability parameter *S* for molecules of resultant complex will increase in comparison with that of free DNA molecules. Let us assume that parameter *S* doubles, then the angle between the long-wavelength ETDM of TPT molecule bound to DNA and the long axis of DNA will change insignificantly, to 59°.

It should be noted that CPT molecule, in contrast to TPT (see Fig. 1), has neither positively charged dimethylaminomethylene group in the 9 position [16] nor hydroxy group in the 10 position. Nonetheless, the long-wavelength ETDMs in CPT and TPT molecules form almost the same angle with the long axis of DNA. CPT and TPT molecules themselves in such complex with DNA seem to be oriented in almost the same manner with respect to the long axis of DNA. Thus both the compounds, in spite of slight difference in structure, appear to form the same type of complex with DNA.

Although the values of angles (57°–59°) obtained in [11] are close to the angles for typical intercalators, $69° \pm 7°$, the authors are disposed to consider that CPT molecule does not intercalate between the base pairs but is positioned in the DNA major groove. The values of angles (62°–64°) obtained by us are in the region of permissible angle values for intercalating molecules.

Nonetheless, we continued to study the orientation of the chromophore of quinoline fragment of TPT molecule with respect to DNA base pairs. We determined the orientations of ETDMs in the quinoline and lactone fragments of TPT molecule using quantum chemical calculations. Figure 4 shows approximate mutual arrangement of the quinoline and lactone fragments in TPT molecule. The dimethylaminomethylene group in the ring A was supposed in calculations to be protonated [16].

ETDM for the quinoline and lactone fragments of TPT molecule were found by quantum chemical calculations. They are presented by vectors in Figs. 4a and 4b, respectively. The strengths of corresponding oscillators are shown by digits in parentheses. Long arrows marked with letter **p** indicate the projections of vectors of static dipoles in the quinoline and lactone fragments of TPT molecule on the plane of corresponding chromophores because they, as distinct from ETDM, are not in these planes but form certain angles with them. This angle is 18° for quinoline fragment, with the vector being directed to the same side as the dimethylaminomethylene group. This angle is –26° for the lactone fragment, with vector pointing away from the deviation of ring E from the plane of ring D.

These results indicate that two long-wavelength ETDMs in the fragments of TPT molecule (at 306 and 302 nm) are virtually parallel to each other. The

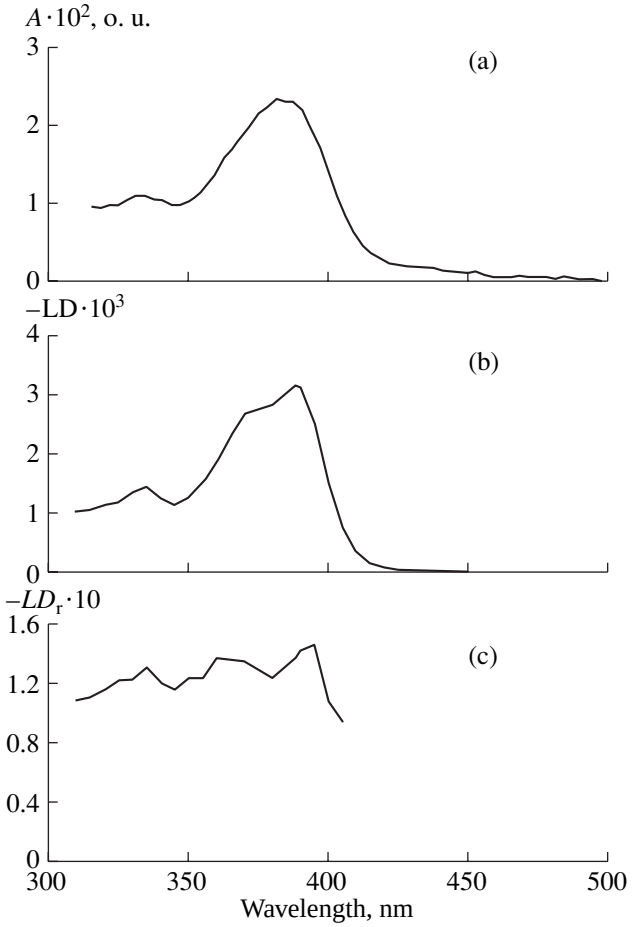

Fig. 3. Absorption spectra (*A*), linear dichroism spectra (*LD*), and reduced linear dichroism spectra (LD_r) for complex of $1.05 \cdot 10^{-5}$ M TPT with $3.5 \cdot 10^{-4}$ M DNA. (a) Absorption spectrum; (b) linear dichroism spectrum; (c) LD_r spectrum; other conditions as in the caption to Fig. 2.

ETDMs of neighboring transitions usually form a considerable angle with each other. But this is true only when the transitions belong to the same chromophore system. In our case, ETDM at 306 nm relates to the chromophore system of the quinoline fragment of TPT molecule, while ETDM at 302 nm pertains to the chromophore system of its lactone fragment. The second ETDM of the quinoline chromophore is only at ~260 nm, which is expected to form an angle of ~100° with its own long-wavelength transition. The calculations were made for vacuum, therefore the calculated wavelengths corresponding to ETDM maxima are shifted to the short-wavelength spectral region as compared with their position observed in experiment. Moreover, the absorption bands of TPT molecule are split probably because of interaction with solvent. The approach used, separation of TPT molecule into two fragments, allowed us to establish that ETDM at 306 nm refers to the quinoline fragment of TPT mol-

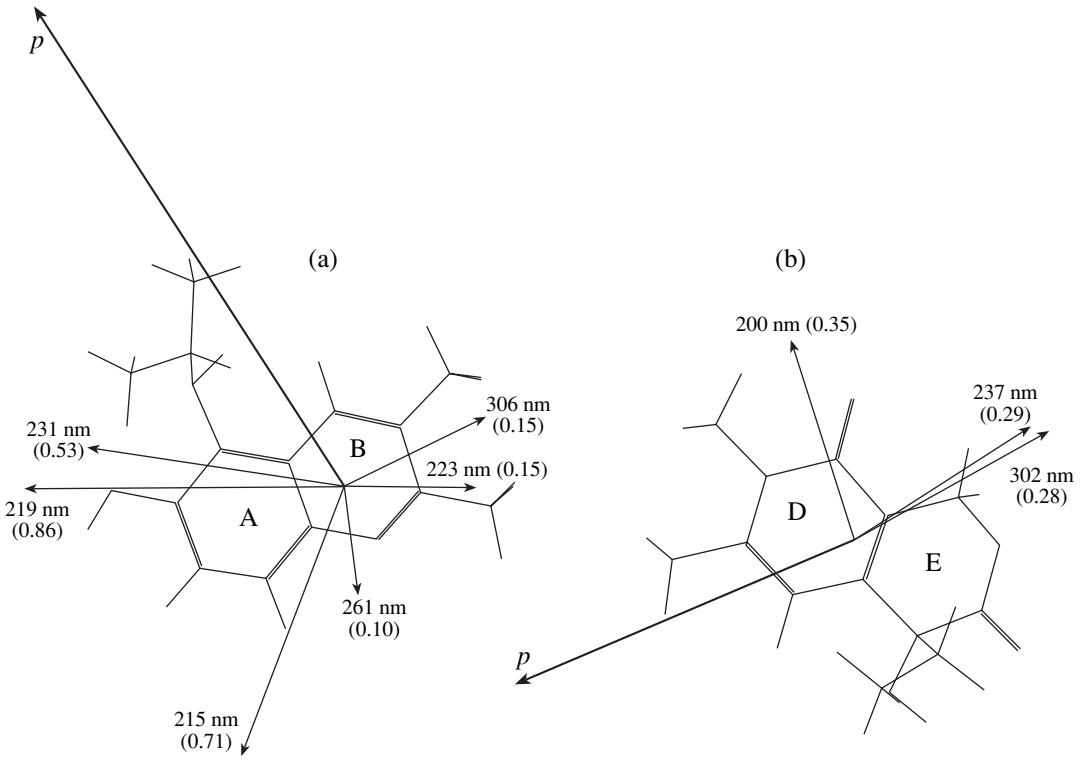

Fig. 4. Orientation of electron transition dipole moments (ETDM) in the fragments of TPT molecule: (a) in quinoline fragment (rings A, B); (b) in lactone fragment (rings D, E). ETDMs are shown by vectors. Neighboring digits in parentheses are the corresponding oscillator strengths. Vectors marked with letter *p* show directions of static dipoles of quinoline and lactone fragments of TPT molecule. Mutual arrangement of these fragments in the figure corresponds approximately their position in TPT molecule.

ecule, while the ETDM at 302 nm belongs to the D ring of the lactone fragment that explains the reason of parallelism of corresponding ETDMs. On the other hand, our previous calculation of TPT molecule as a whole (see Fig. 6a in work [16]) showed that the directions of long-wavelength ETDMs to the first approximation were virtually the same as those for the lactone and quinoline fragments separately. Such a coincidence is a good verification for the applicability of this quantum chemical method.

For comparison with quantum chemical calculations, Fig. 5 shows absorption spectra of TPT: curve *1* for free and curve *2* for bound compound. In both cases, TPT concentration was $9.9 \cdot 10^{-6}$ M, and DNA concentration was $3.6 \cdot 10^{-4}$ M. According to [1], DNA is completely filled with TPT molecules under these conditions. Indeed, free TPT shows absorption bands in the regions 370–390, 320–330, 260–280 and 220 nm, which agree well with the data obtained by quantum chemical calculations (see Fig. 4). The comparison of the absorption spectra of free and bound TPT (see Fig. 5, curves *1* and *2*, respectively) indicates negligible alteration of the long-wavelength absorption band of TPT upon formation of TPT–DNA complex. We assume this is true also for the short-wavelength absorption bands of TPT.

Although LD_r values and corresponding to them angles were determined in sufficiently wide spectral range from 310 to 410 nm, we could find angle only between virtually parallel long-wavelength ETDMs (at 327 and 382 nm, see Fig. 5) rather than between the plane of quinoline chromophore and the long axis of DNA molecule. This is illustrated by Fig. 6a where rectangle represents schematically a TPT molecule whose one of ETDMs designated by letter C forms with the polymer long axis designated by F an angle of 90°, although the ligand plane is *parallel* to the polymer long axis. On the other hand, it is known from geometry that only perpendicular to two crossed lines laying in a plane is perpendicular to the plane. This is illustrated by Fig. 6b. The polymer long axis designated by letter F forms right angles with two crossed ETDMs of TPT molecule designated by letters C and D, hence the polymer long axis and the TPT chromophore plane will also form right angle.

To answer the question on the orientation of the quinoline chromophore plane of TPT molecule with respect to the long axis of DNA, we had to study the short-wavelength region of TPT spectrum where it

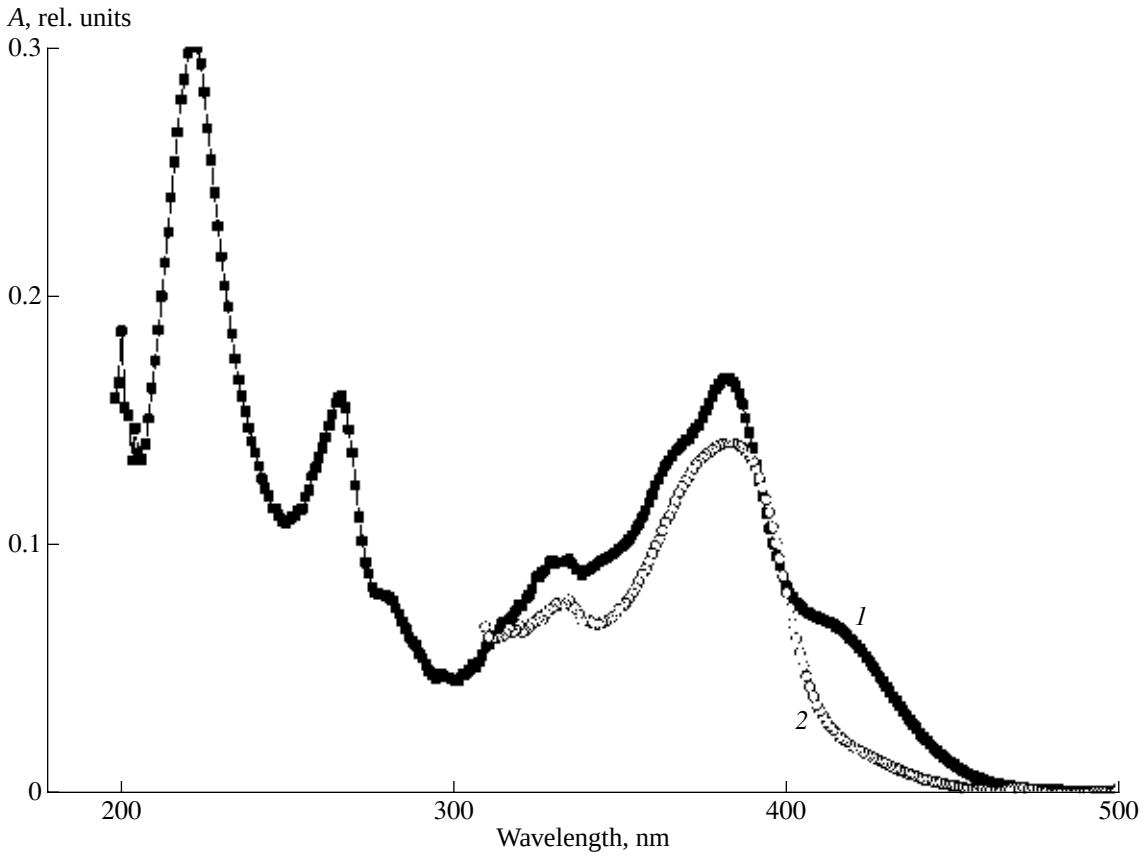

Fig. 5. Absorption spectra of free and bound to DNA TPT. Spectrum *1*, free TPT ($9.9 \cdot 10^{-6}$ M); spectrum *2*, complex containing $9.9 \cdot 10^{-6}$ M TPT and $3.6 \cdot 10^{-4}$ M DNA. Optical path length of cuvette is 1 cm. Buffer as in the caption to Fig. 2.

overlapped with the absorption band of DNA bases. This task is complicated by several circumstances.

We have shown earlier that at least three days are necessary for the formation of the studied type of TPT–DNA complex [1]. Moreover, it was found in [4] that CPT close in structure to TPT could cleave sugar–phosphate backbone upon interaction with ring supercoiled DNA (observations were accomplished in 6 h after complex preparation). This cleavage may cause a shortening of DNA molecule and hence decrease in its LD owing to reduction of orientation ability parameter *S* of macromolecule. This effect may be avoided if LD is measured immediately after TPT addition to DNA. This leads to the loss of quantitative (incomplete TPT binding to DNA) but not qualitative assessment of LD alteration upon TPT binding to DNA. Figure 7 shows dependence of LD values measured at 280 and 390 nm (curves *1* and *2*, respectively) on the time of complex formation at concentrations $4.04 \cdot 10^{-5}$ M DNA and $9.92 \cdot 10^{-5}$ M TPT. According to [1], the binding of TPT is maximal under these conditions.

The experiment lasted for about 45 min, the measurements were carried out discretely each 5 min, a solution of TPT–DNA complex was kept in the dark between the measurements. Therefore DNA decomposition in the presence of TPT is very unlikely over such a short time. Figure 7 (curve *2*) shows both the growth of LD amplitude at 390 nm and its drop at

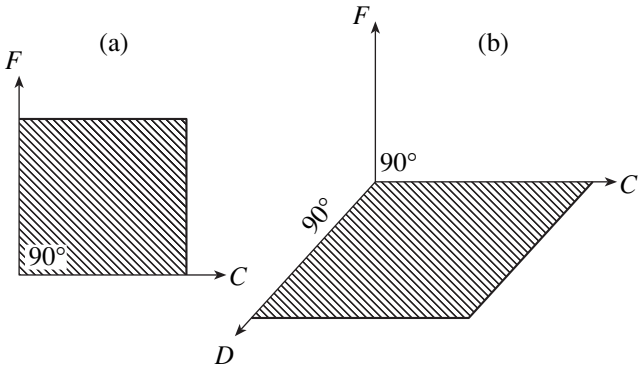

Fig. 6. Two possible orientations of polymer long axis relative to ETDM of TPT molecule. (a) The long axis (*F*) of polymer is perpendicular to *C*, one ETDM of TPT molecule. (b) The long axis (*F*) of polymer is perpendicular to *C* and *D*, two intersecting ETDMs of TPT molecule. The plane of TPT chromophore is shaded.

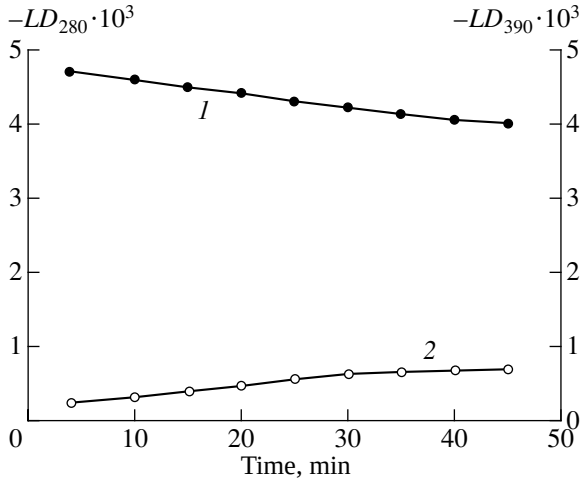

Fig. 7. Dependence of LD values of TPT–DNA complex measured at 280 and 390 nm on the time of complex formation. Curve *1* is the dependence of LD_{280} (left axis); curve *2* is the dependence of LD_{390} (right axis). The complex contained $4.04\cdot10^{-5}$ M DNA and $9.92\cdot10^{-5}$ M TPT. Other conditions as in the caption to Fig. 2.

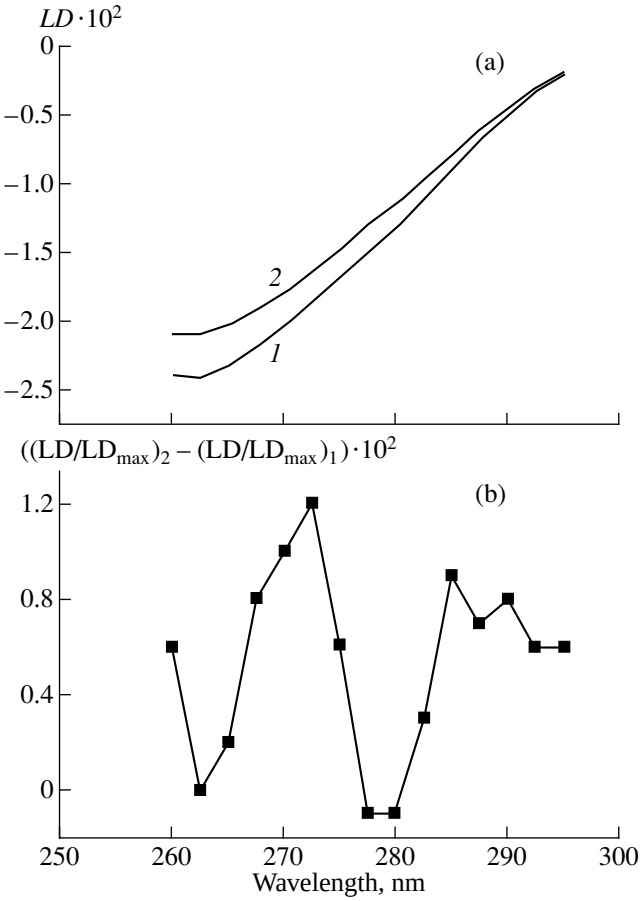

Fig. 8. (a) LD spectra of DNA in the absence (*1*) and in the presence of TPT (*2*). (b) Difference spectrum between LD spectrum of TPT–DNA complex and LD spectrum of free DNA normalized by their maximal values. Free DNA concentration is $2.94\cdot10^{-4}$ M. The complex contained $2.94\cdot10^{-4}$ M DNA and $1.7\cdot10^{-5}$ M TPT. Other conditions as in the caption to Fig. 2.

280 nm (curve *1*). The growth of the amplitude of LD signal at 390 nm is known to reflect TPT–DNA complex formation. It is naturally to assume that the drop in the amplitude of LD signal at 280 nm is explained by the same reason.

One can suppose several reasons to explain the drop in the amplitude of LD signal at 280 nm upon TPT–DNA complex formation, namely: (1) change in the inclination angle of DNA bases with respect to the long axis of DNA (angle α in formula 1), (2) decrease in the orientation ability of TPT–DNA complex as compared with free DNA (reduction of parameter *S* in formula 1), although this explanation is unlikely because the complexation of TPT with DNA appears to be accompanied by association of several DNA molecules with each other [1] and hence the orientation ability of such a complex must increase; (3) a contribution of positive LD signal corresponding to bound TPT molecules.

If two first assumptions are true, the LD spectrum of TPT–DNA complex should be similar to that of free DNA in accordance with formula 1, i.e., $LD_1 = \beta\cdot LD_2$, where indices 1 and 2 refer to free DNA and its complex with TPT, while β is a proportionality factor. This equality is valid for all wavelengths within this region including the corresponding spectral maxima: $LD_{max,\,1} = \beta\cdot LD_{max,\,2}$. Let us normalize each of spectra by its maximal value and subtract first normalized spectrum from the second one to produce $LD_2/LD_{max,\,2} - LD_1/LD_{max,\,1}$. Replacement of LD_1 in this expression by $\beta\cdot LD_2$ and $LD_{max,\,1}$ by $\beta\cdot LD_{max,\,2}$ will result in zero. If the third assumption is true, the shape of normalized LD spectrum of TPT–DNA complex has to differ from the shape of normalized spectrum of free DNA and the above manipulation will not produce zero. To ascertain which of these assumptions is true, first we recorded the LD spectrum of free DNA at concentration of $2.94\cdot10^{-4}$ M (Fig. 8a, curve *1*), then a small portion (1:45 by volume) of TPT at concentration of $8.25\cdot10^{-4}$ M was added (to concentration $1.7\cdot10^{-5}$ M in solution) so that the dilution of DNA could be neglected and LD spectrum was recorded again (Fig. 8a, curve *2*). Both the spectra were normalized by their maximal magnitudes. Then normalized spectrum *1* was subtracted from normalized spectrum *2*. The resultant LD spectrum is shown in Fig. 8b. We must remind that the amplitudes of normalized spectra are within the range from 0 to 1, and therefore the difference between these spectra is far less. There is no statistical spread of points in Figure 8b in the neighborhood of zero point as would be expected if the first two assumptions prove to be valid. The figure shows

two positive maxima at 272 and 285 nm. Let us compare this spectrum with that of free TPT shown in Fig. 5. The latter has a maximum at ~265 nm and a shoulder at ~275 nm. Since a slight bathochromic shift is observed in spectrum of TPT upon its interaction with DNA (see Fig. 5), which is evident from the long-wavelength band of TPT, we may consider as a very good coincidence the bands at 265 nm of TPT absorption spectrum (see Fig. 5) and at 272 nm from the LD difference spectrum (see Fig. 8b) as well as the bands at 275 nm (see Fig. 5) and 285 nm (see Fig. 8b). Thus, a superposition of the positive LD signal from TPT molecules bound to DNA on the negative LD signal from DNA takes place in the region 260–295 nm upon TPT addition to DNA.

This confirms the above assumption that positive LD value from bound TPT molecules reduces the amplitude of total LD signal in the region 260–295 nm. Consequently, the short-wavelength ETDMs of bound TPT molecule form angle *less* than 54° with the long axis of DNA. Then, the angle between the plane of the quinoline chromophore of TPT molecule and the long axis of DNA is not larger. The molecules having such a position of chromophore plane with respect to the long axis of DNA *cannot* intercalate between nucleotide pairs of DNA because this angle α cannot be lesser 60° for any known intercalators. Indeed, the value of angle α for typical intercalators is 70° for ethidium bromide, 82° for proflavine, and 61° for actinomycin D [12].

Thus, in the case of TPT binding to DNA, there is such a disposition of ligand molecule relative to DNA base pairs when one ETDM in TPT molecule lays virtually in the plane of bases, whereas another forms a considerable angle with this plane.

Such an arrangement of TPT molecule with respect to the long axis of DNA is unusual but not unique. Similar orientation, having negative LD in one absorption band of bound ligand and positive LD in another band, was observed by us for furan analog of distamycin A [26] and by Nordén for methyl green [27].

This arrangement of ETDM in TPT molecule may result (upon analysis of only long-wavelength region of spectra of TPT molecule bound to DNA) in erroneous conclusion on the intercalation of this molecule between DNA base pairs because induced CD of negative sign is observed for this molecule upon binding to DNA. As a matter of fact, the negative sign of induced CD indicates only that the direction of the corresponding long-wavelength ETDM in bound molecule almost coincide with the twofold symmetry axis of DNA molecule directed to the minor groove of the polymer [28]. Nonetheless, ligand molecule itself may be turned around this axis with respect to the plane of DNA bases by significant angle like in the case of TPT molecule.

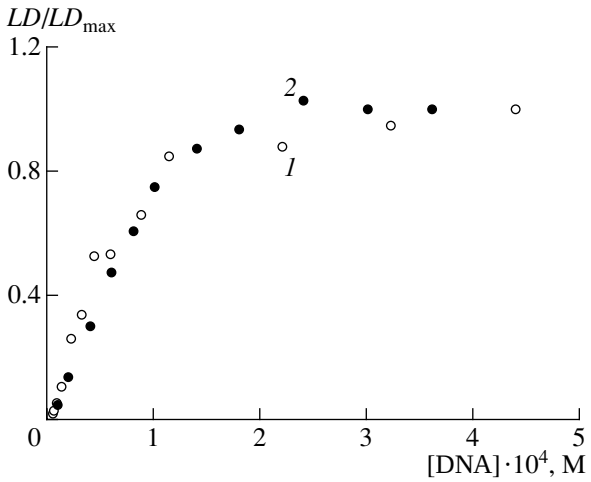

Fig. 9. Dependence of the share of TPT bound to DNA (LD/LD_{max}) on DNA concentration in solution. *1* (light circles), calf thymus DNA; *2* (black circles), coliphage T4 DNA. Solutions contained $1.36 \cdot 10^{-5}$ M TPT. Other conditions as in the capture to Fig. 2.

Upon binding of CPT family molecules to DNA, a number of authors [4, 6] observed hypochromic effect (see, for example, Fig. 5) also in the long-wavelength absorption band of this ligand. This effect may be caused both by interaction of virtually parallel to each other ETDMs of the ligand and base pair and by a shift of monomer–dimer equilibrium for TPT molecules toward larger dimer formation in the presence of DNA, which is also accompanied by hypochromic effect [16]. Consequently, the hypochromic effect in the DNA absorption band also can not serve as unambiguous evidence for the intercalation of TPT molecule.

Thus, the results obtained indicate the lack of intercalation of TPT molecule between DNA base pairs, moreover, they provide a possibility to explain the data obtained previously by other authors [4, 6, 11] without using the intercalation hypothesis.

TPT does not bind in the DNA major groove. To refine the TPT localization on DNA, we compared the curves of TPT binding to calf thymus DNA and coliphage T4 DNA obtained by LD measurements at 390 nm. In coliphage T4 DNA, all cytosines at the 5th position are known to be linked to glucose residues [29], which are disposed in the DNA major groove and prevent binding to any ligand at this groove. To obtain binding curves, portions of concentrated solution of these DNAs were added to TPT at concentration $1.36 \cdot 10^{-5}$ M and LD values were measured at 390 nm. The addition of DNA was continued until both the dependences reach a plateau, i.e., until all TPT became bound to DNA. Since these DNAs has different length, the obtained dependences were normalized by their maximal values for convenience in

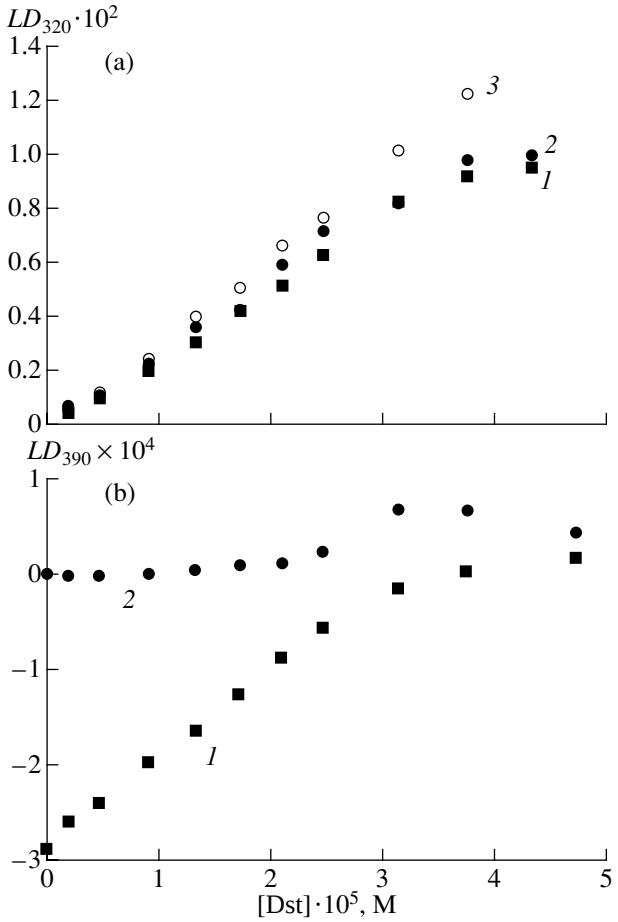

Fig. 10. a and b are dependences of LD_{320} and LD_{390}, respectively, for TPT–DNA complexes and free DNA on Dst concentration in solution. *1* (black squares), complex of $1.05 \cdot 10^{-5}$ M TPT with $1.15 \cdot 10^{-4}$ M DNA; *2* (black circles), $1.15 \cdot 10^{-4}$ M DNA; *3* (light circles), $4.13 \cdot 10^{-4}$ M DNA. Other conditions as in the caption to Fig. 2.

comparing the binding curves with each other. Figure 9 shows these curves in the normalized view (LD/LD_{max}). Curve *1* and curve *2* correspond to TPT binding to calf thymus DNA and to coliphage T4 DNA, respectively. Both the curves have the same S-shaped profile and coincide with each other. If TPT molecules are located only in the DNA major groove upon binding, so no binding at all would be observed to coliphage T4 DNA. If both the grooves are equally available for TPT binding, then the inaccessibility of the major groove of coliphage T4 DNA would result in a right shift of the curve for coliphage T4 DNA relative to the curve for calf thymus DNA because twofold concentration of coliphage T4 DNA would be necessary to equalize the number of potential binding sites on these DNAs.

The coincidence of TPT binding curves for coliphage T4 DNA and calf thymus DNA indicates that the DNA major groove does not participate in TPT binding.

Competition of TPT with distamycin A for binding sites in the minor groove of both DNA and poly(dG-dC)·poly(dG-dC). To reveal the role of the DNA minor groove in the TPT interaction with DNA, we studied the competition between distamycin antibiotic and TPT for binding sites on DNA because Dst is known as a ligand that combines with DNA at the minor groove with high binding constant [30]. The LD spectrum of Dst bound to DNA has positive sign [31], its maximum is at 320 nm, i.e., in the shorter wavelength region in comparison with the maximum of TPT bound to DNA (390 nm) that enables independent detection of interaction of two these compounds with DNA by LD method.

In order to determine whether Dst and TPT molecules compete for binding sites on DNA, portions of concentrated Dst solution were added to solutions of calf thymus DNA at concentrations of $4.13 \cdot 10^{-4}$ M and $1.15 \cdot 10^{-4}$ M in a free state and as the complex containing $1.15 \cdot 10^{-4}$ M DNA and $1.05 \cdot 10^{-5}$ M TPT and LD values were measured at 320 and 390 nm. The obtained dependences of LD_{320} and LD_{390} on Dst concentration are shown in Figs. 10a and 10b, respectively. Curve *1* refers to TPT–DNA complex, curve *2* relates to DNA at concentration $1.15 \cdot 10^{-4}$ M, and curve *3* corresponds to $4.13 \cdot 10^{-4}$ M DNA. Curves *3* and *2* in Fig. 10a virtually coincide throughout the range of concentrations until curve *2* reaches a plateau. Since DNA concentrations for these curves differ by a factor of about 4, such behavior of the curves indicates that all added Dst binds to DNA. Thus, there is a high constant of Dst binding to DNA that agree well with literature data [32]. Curve *2* reaches the plateau at Dst concentration of $3.3 \cdot 10^{-5}$ M, i.e., at the ratio one added (and as follows from above one bound) Dst molecule per 2.8 bp of DNA, which is consistent with data from [21]. One Dst molecule occupies 5 bp of DNA on monomeric binding [33, 34], consequently the obtained result indicates preferably dimeric binding of Dst to DNA under our conditions.

All three curves shown in Fig. 10a have a slighty S-shaped profile indicating the low cooperativity of Dst binding to DNA [35]. Curve *1* obtained upon addition of Dst to TPT–DNA complex reaches a saturating level corresponding to 2.6 bp of DNA per one bound Dst molecule, i.e., virtually at the same Dst to DNA concentration ratio as in the absence of TPT. The saturating level for curves *2* and *1* is almost the same. The coincidence of curves *1* and *2* could be explained by almost the same amount of bound Dst in both cases, i.e., complete displacement of TPT into solution. This result agrees well with the fact that the addition of Dst to TPT–DNA complex causes complete disappearance of LD signal at 390 nm corresponding to bound TPT, see Fig. 10b, curve *1*. Curve *2* in Fig. 10b demonstrates the contribution to LD at 390 nm of Dst bound to free DNA. The observed alter-

ations in LD value are minor in comparison with alteration in LD at 390 nm upon addition of Dst to TPT–DNA complex, therefore the behavior of curve *1* is explained by the displacement of TPT from DNA by Dst molecules rather than by the result of algebraic summation of LD signals of TPT and Dst having opposite signs. Thus, the presence of TPT bound to DNA does not prevent its binding to Dst because the addition of Dst appears to cause complete displacement of TPT from DNA.

Alternative explanation of these facts may consist in that Dst molecules do not bind at all to those base sequences where TPT does. This assumption makes it possible to explain the same saturating level in curves *1* and *2* (Fig. 10a) but cannot explain why the addition of Dst results in disappearance of LD signal at 390 nm in the absorption band of bound TPT (Fig. 10b). To explain this fact, we have to add "one more epicycle" to our assumptions, i.e., supposition that the disappearance of LD signal at 390 nm is not caused by TPT displacement from DNA but results from such an alteration of spatial orientation of TPT molecule at which LD value at 390 nm converts to zero according to formula 1. This transformation occurs only for the orientation of bound TPT molecules and has no effect on the orientation of Dst molecules bound to DNA. Indeed, the retention of saturating level toward LD for Dst molecule in the presence and in the absence of TPT indicates that the orientation of ETDM at 320 nm for bound Dst molecules with respect to the long axis of DNA does not change even upon possible alteration in the orientation of bound TPT molecule. However, the LD spectrum of Dst contains an additional absorption band at ~260 nm which refers to another transition in this molecule [26]. The coincidence of not only saturating level at one wavelength but a full spectrum composed at least of two transitions evidences the constant orientation of entire Dst molecule in the presence and in the absence of TPT in solution. Indeed, the LD spectra of Dst in the presence (curve *1*) and in the absence of TPT molecules in solution (curve *2*) coincide with each other, see Fig. 11. Thus, only displacement of TPT molecules from DNA by Dst molecules can explain all experimental data.

Let us continue to consider the result shown in Fig. 10b. Curve *2* in Fig. 10b in contrast to curve *2* in Fig. 10a has obvious S-shaped character, which appears only at high filling of DNA with Dst. We suppose the S-shaped character of the curve of Dst binding to DNA may be brought about by several reasons. Upon binding to different sequences of base pairs, Dst can have slightly different LD spectra, cooperativity parameters, and binding constants [30]. Therefore initially Dst will fill AT-reach DNA sites and then GC-reach ones. Indeed, the binding constant of Dst to ATTA sequence is $2.5 \cdot 10^7$ M^{-1}, whereas that to AGGA is only $1.8 \cdot 10^5$ M^{-1} [36]. Note that Dst binding

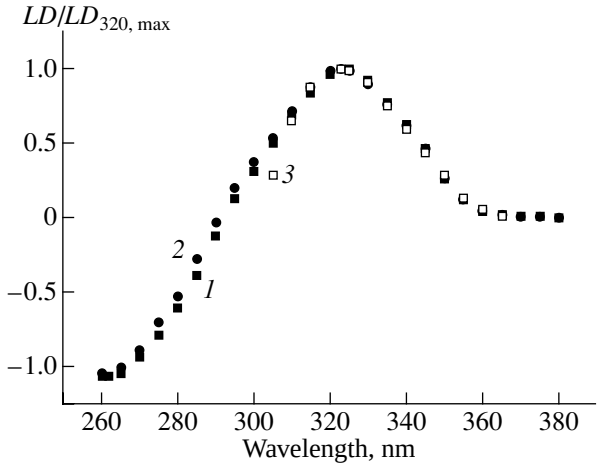

Fig. 11. LD spectra of free calf thymus DNA, TPT complex with calf thymus DNA, and TPT complex with poly(dG-dC)·poly(dG-dC) in the presence of saturating concentrations of Dst. The spectra are normalized by the $LD_{320, max}$ value. *1* (black squares), complex of $1.05 \cdot 10^{-5}$ M TPT with $1.15 \cdot 10^{-4}$ M DNA in the presence of $4.32 \cdot 10^{-5}$ M Dst; *2* (black circles), $1.15 \cdot 10^{-4}$ M DNA in the presence of $4.32 \cdot 10^{-5}$ M Dst; *3* (light squares), complex of $1.05 \cdot 10^{-5}$ M TPT with $8.73 \cdot 10^{-5}$ M poly(dG-dC)·poly(dG-dC) in the presence of $5.33 \cdot 10^{-5}$ M Dst. Other conditions as in the capture to Fig. 2.

constant rises when solution ionic strength decreases [37], this is essential for our experiments accomplished in 1 mM sodium cacodylate.

We studied Dst binding to poly(dG-dC)·poly(dG-dC) in the absence and in the presence of TPT in solution to verify the above rather unusual assumption that TPT molecules, being bound to DNA, change their spatial orientation in the presence of Dst so as not to appear in LD at 390 nm. For this purpose, portions of Dst were added to solutions of free poly(dG-dC)·poly(dG-dC) at concentrations of $8.73 \cdot 10^{-5}$ M and $4.36 \cdot 10^{-5}$ M and a complex solution containing $8.73 \cdot 10^{-5}$ M poly(dGdC)·poly(dG-dC) and $1.05 \cdot 10^{-5}$ M TPT and LD values at 320 and 390 nm were measured. Curve *1* relates to the complex of $8.73 \cdot 10^{-5}$ M poly(dG-dC)·poly(dG-dC) with $1.05 \cdot 10^{-5}$ M TPT, curve *2* refers to $4.36 \cdot 10^{-5}$ M poly(dG-dC)·poly(dG-dC), and curve *3* corresponds to $8.73 \cdot 10^{-5}$ M poly(dG-dC)·poly(dG-dC). The results of LD measurements at 320 and 390 nm are shown in Fig. 12a and Fig. 12b, respectively. The addition of Dst to free poly(dG-dC)·poly(dG-dC) led to appearance of positive LD signal at 320 nm and almost complete coincidence of spectra of Dst bound to calf thymus DNA and to poly(dG-dC)·poly(dG-dC) (see Fig. 11, spectra *1* and *3*). Hence, Dst binding to the minor groove of polydeoxyribonucleotide takes place also for poly(dG-dC)·poly(dG-dC).

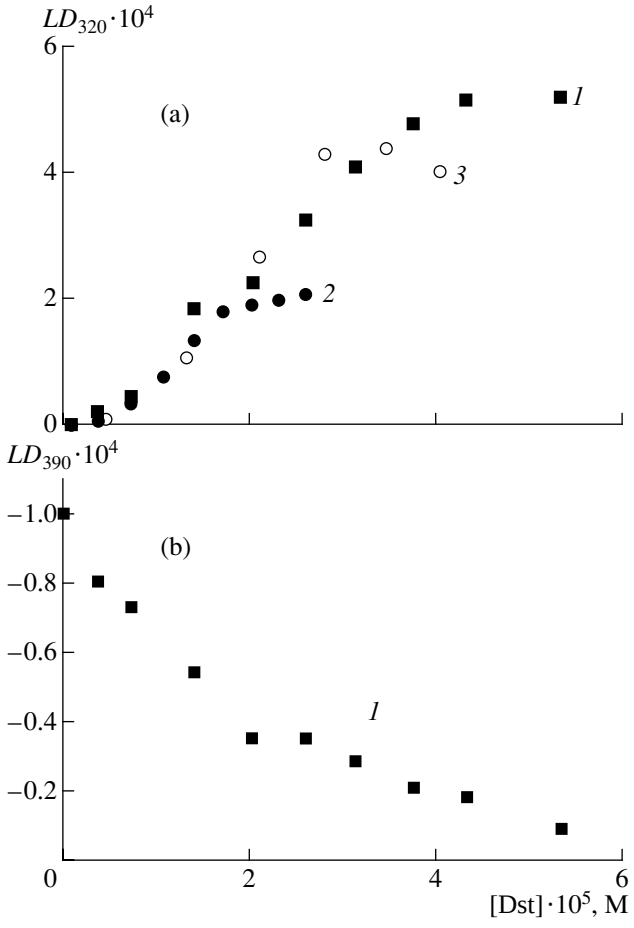

Fig. 12. a and b are dependences of LD_{320} and LD_{390}, respectively, for TPT–poly(dG-dC)·poly(dG-dC) complex and free poly(dG-dC)·poly(dG-dC) on Dst concentration in solution. *1* (black squares), complex of $1.05 \cdot 10^{-5}$ M TPT with $8.73 \cdot 10^{-5}$ M poly(dG-dC)·poly(dG-dC); *2* (black circles), $4.36 \cdot 10^{-5}$ M poly(dG-dC)·poly(dG-dC); *3* (light circle), $8.73 \cdot 10^{-5}$ M poly(dG-dC)·poly(dG-dC). Other conditions as in the caption to Fig. 2.

Let us note two features of Dst binding to poly(dG-dC)·poly(dG-dC) in a free state and in complex with TPT.

(1) A very weak positive band at 390 nm appears in the LD spectrum of bound Dst (the spectrum not shown) similar to that observed upon addition of Dst to calf thymus DNA (see Fig. 10b).

(2) When the ratio of added Dst to poly(dG-dC)·poly(dG-dC) is 1 Dst molecule per 5 bp, slow variation of LD signal proceeds in solution: initially, after Dst addition, the signal drops almost to zero and then comes slowly to its equilibrium magnitude. These features of Dst binding require special investigation.

Curves *3* and *2* obtained at different polymer concentrations (until curve *2* achieves saturation level, see Fig. 12a) differ negligibly that indicates that virtually all added Dst binds to the polymer under these conditions. That is, Dst shows sufficiently high binding constant again but with poly(dG-dC)·poly(dG-dC) in this case. Therefore the stoichiometry of Dst binding to poly(dG-dC)·poly(dG-dC) can be estimated from the saturating level of curves *2* and *3*. It was found that one Dst molecule binds to 2.5 bp of polymer, which testifies to the dimeric character of Dst binding to poly(dG-dC)·poly(dG-dC). Curves *1–3* shown in Fig. 12a have more pronounced S-shaped profile than in Fig. 10a, which indicates much more prominent cooperativity of formation of Dst dimer on GC-rich domains as compared with AT-rich regions of the double-helical polynucleotide [38]. It becomes clear therefore why cooperativity upon LD measurements at 390 nm was detected when larger amount of Dst was added upon titration of calf thymus DNA by Dst, i.e., when Dst began to bind to GC-rich DNA sites.

Curve *1* corresponding to Dst binding to poly(dG-dC)·poly(dG-dC) in the presence of TPT and curve *3* corresponding to Dst binding to the free polymer have almost the same saturating level. This indicates that the amount of bound Dst is close in both cases, i.e., Dst completely displaces TPT from poly(dG-dC)·poly(dG-dC). This is also evidenced by the behavior of curve *1* in Fig. 12b: as Dst was added to TPT–poly(dG-dC)·poly(dG-dC) complex, the LD_{390} value (indicating the quantity of TPT bound to the DNA) decreased to zero.

Finally, it should be emphasized that human topo I, whose inhibitor is TPT, also forms contacts with the DNA minor groove in the region of phosphodiester bond cleavage [39]. Such coincidence of DNA binding sites for enzyme and TPT appears to be necessary for the functioning of CPT family molecules as topo I inhibitors.

CONCLUSIONS

The study of TPT binding to calf thymus DNA and coliphage T4 DNA as well as competition of TPT with Dst for binding sites on DNA and on poly(dG-dC)·poly(dG-dC) allows us to make the following conclusions:

(1) the TPT molecule does not intercalate between DNA base pairs,

(2) the TPT molecule does not interact with the DNA major groove,

(3) the TPT molecule competes with Dst for binding sites in the minor groove of DNA and poly(dG-dC)·poly(dG-dC).

Thus, it has been shown for the first time that TPT, a member of CPT family, binds to double-stranded DNA at the minor groove upon complexation.

We will note that the above is true for specific type of TPT–DNA complexes, namely for complex having negative LD at 390 nm, where DNA molecules combine with each other in the presence of TPT molecules [1].

ACKNOWLEDGMENTS

This work was supported by the Russian Foundation for Basic Research (projects nos. 01-04-48657, 01-03-32669, and 00-15-97834) and INTAS (project no. 97-0522).

REFERENCES

1. Strel'tsov, S.A., Mikheikin, A.L., and Nechipurenko, Yu.D., *Mol. Biol.*, 2001, vol. 35, pp. 442–450.
2. Wall, M.E., Wani, M.C., Cook, C.E., Palmer, K.H., McPhail, A.T., and Sim, G.A., *J. Am. Chem. Soc.*, 1966, vol. 88, pp. 3888–3890.
3. Horwitz, S.B., Chang, C.K., and Grollman, A.P., *Mol. Pharmacol.*, 1971, vol. 7, pp. 632–644.
4. Fukada, M., *Biochem. Pharmacol.*, 1985, vol. 34, pp. 1225–1230.
5. Leteurtre, F., Fesen, M., Kohlhagen, G., Kohn, K.W., and Pommier, Y., *Biochemistry*, 1993, vol. 32, pp. 955–962.
6. Yang, D., Strode, J.T., Spielmann, H.P., Wang, A.H.-J., and Burke, T.G., *J. Am. Chem. Soc.*, 1998, vol. 120, pp. 2979–2980.
7. Hertzberg, R.P., Caranda, M.J., and Hecht, S.M., *Biochemistry*, 1989, vol. 28, pp. 4629–4638.
8. Hsiang, Y.H., Hertzberg, R., Hecht, S., and Liu, L.F., *J. Biol. Chem.*, 1985, vol. 260, pp. 14873–14878.
9. Jaxel, C., Kohn, K.W., Wani, M.C., Wall, M.E., and Pommier, Y., *Cancer Res.*, 1989, vol. 49, pp. 1465–1469.
10. Fan, Y., Weinstein, J.N., Kohn, K.W., Shi, L.M., and Pommier, Y., *J. Med. Chem.*, 1998, vol. 41, pp. 2216–2226.
11. Bailly, C., Riou, J.-F., Colson, P., Houssier, C., Rodrigues-Pereira, E., and Prudhomme, M., *Biochemistry*, 1997, vol. 36, pp. 3917–3929.
12. Hogan, M., Dattagupta, N., and Crothers, D.H., *Biochemistry*, 1979, vol. 18, pp. 280–288.
13. Bailly, C., Hinichart, J.-P., Colson, P., and Houssier, C., *J. Mol. Recognit.*, 1992, vol. 5, pp. 155–171.
14. Lyng, R., Rodger, A., and Nordén, B., *Biopolymers*, 1992, vol. 32, pp. 1201–1214.
15. Yao, S., Murali, D., Sectharamulu, P., Harides, K., Petluru, P.N.V., Reddy, D.G., and Hausheer, F.H., *Cancer Res.*, 1998, vol. 58, pp. 3782–3788.
16. Strel'tsov, S.A., Grokhovsky, S.L., Kudelina, I.A., Oleinikov, V.A., and Zhuze, A.L., *Mol. Biol.*, 2001, vol. 35, pp. 432–441.
17. Zasedatelev, A.S., Gurskii, G.V., and Vol'kenshtein, M.V., *Mol. Biol.*, 1971, vol. 5, pp. 245–251.
18. McGhee, J.D. and von Hippel, P.H., *J. Mol. Biol.*, 1974, vol. 86, pp. 469–489.
19. Wells, R.D., Larson, J.E., Grant, R.C., Shortle, B.E., and Cantor, C.R., *J. Mol. Biol.*, 1970, vol. 54, pp. 465–497.
20. Votavova, H., Burckhardt, G., Sponar, J., and Zimmer, C., *Biochim. Biophys. Acta*, 1981, vol. 654, pp. 175–180.
21. Luck, G., Zimmer, Ch., Reinert, K.-E., and Arcamone, F., *Nucleic Acids Res.*, 1977, vol. 4, pp. 2655–2670.
22. Makarov, V.L., Strel'tsov, S.A., Vengerov, Yu.Yu., Khorlin, A.A., and Gurskii, G.V., *Mol. Biol.*, 1983, vol. 17, pp. 1089–1101.
23. Nordén, B., *Appl. Spectr. Rev.*, 1978, vol. 14, pp. 157–284.
24. Nabiev, I., Fleury, F., Kudelina, I., Pommier, Y., Charton, F., Riou, J.-F., Alix, A.J.P., and Manfait, M., *Biochem. Pharmacol.*, 1998, vol. 55, pp. 1163–1174.
25. Zerner, M.C., Loew, G.H., Kirchner, R.F., and Mueller-Westerhoff, U.T., *J. Am. Chem. Soc.*, 1980, vol. 102, pp. 589–599.
26. Mikheikin, A.L., Nikitin, A.M., Strel'tsov, S.A., Leinsoo, T.A., Chekhov, V.O., Brusov, R.V., Zhuze, A.L., Gurskii, G.V., Shafer, R., and Zasedatelev, A.S., *Mol. Biol.*, 1997, vol. 31, pp. 1002–1011.
27. Kim, S.K. and Nordén, B., *FEBS Lett.*, 1993, vol. 315, pp. 61–64.
28. Lyng, R., Rodger, A., and Nordén, B., *Biopolymers*, 1991, vol. 31, pp. 1709–1720.
29. Lehman, I.R. and Pratt, E.A., *J. Biol. Chem.*, 1960, vol. 235, pp. 3254–3259.
30. Zimmer, Ch. and Luck, G., *FEBS Lett.*, 1970, vol. 10, pp. 339–342.
31. Sveshnikov, P.G., Grokhovsky, S.L., Zhuze, A.L., Kondrat'eva, N.O., Makarov, V.L., and Poletaev, A.I., *Mol. Biol.*, 1978, vol. 12, pp. 557–564.
32. Zimmer, Ch. and Wahnert, U., *Prog. Biophys. Mol. Biol.*, 1986, vol. 47, pp. 31–112.
33. Zasedatelev, A.S., Zhuze, A.L., Tsimmer, K., Grokhovsky, S.L., Tumanyan, V.G., Gurskii, G.V., and Gottikh, B.P., *Dokl. Akad. Nauk SSSR*, 1976, vol. 231, pp. 1006–1009.
34. Zasedatelev, A., Zhuze, A., Zimmer, Ch., Grokhovsky, S.L., Tumanyan, V., Gursky, G., and Gottikh, B., *Studia Biophysica*, 1978, vol. 67, pp. 47–48.
35. Pelton, J.G. and Wemmer, D.E., *Proc. Natl. Acad. Sci. USA*, 1989, vol. 86, pp. 5723–5727.
36. Baliga, R. and Crothers, D.M., *J. Am. Chem. Soc.*, 2000, vol. 122, pp. 11751–11752.
37. Zasedatelev, A.S., Gursky, G.V., Zimmer, Ch., and Thrum, H., *Mol. Biol. Reports*, 1974, vol. 1, pp. 337–342.
38. Fagan, P. and Wemmer, D.E., *J. Am. Chem. Soc.*, 1992, vol. 114, pp. 1080–1081.
39. Redinbo, M.R., Stewart, L., Kuhn, P., Champoux, J.J., and Hol, W.G.J., *Science*, 1998, vol. 279, pp. 1504–1513.